

## Neutron resonance spectroscopy: $^{139}\text{La}^\dagger$

G. Hacken, J. Rainwater, H. I. Liou,\* and U. N. Singh

Columbia University, New York, New York 10027

(Received 26 January 1976)

Results of high resolution neutron time of flight spectroscopy measurements on natural lanthanum (99.9%  $^{139}\text{La}$ ) are presented. Plots of  $\sigma_t$  vs  $E$  are given to 76 keV. Values of  $E_0$  and  $g\Gamma_n^0$  are presented for all 150  $^{139}\text{La}$  levels observed to 26 keV. About 50 of these levels are probably  $p$  levels, based on Bayes' theorem and the minimum  $g\Gamma_n^0$  for detection vs  $E$ . Intermediate structure seems to be present in  $S_0 \equiv \sum g\Gamma_n^0/\Delta E$ . From 6 to 18 keV,  $10^4 S_0 \approx 0.50$ . Two strong levels at 3 and 3.5 keV, and several strong levels in the 18.5 to 26 keV region, boost  $S_0$  to a value  $10^4 S_0 = 0.76$  for the full 26 keV range. A standard analysis that ignores intermediate structure and uses a single channel Porter-Thomas fit to the entire  $g\Gamma_n^0$  population yields  $10^4 S_0 = 0.76 \pm 0.13$ ,  $D_0 = 208 \pm 10$  eV, and  $10^4 S_1 = (0.6_{-0.2}^{+0.3})$ .

[ NUCLEAR REACTIONS  $^{139}\text{La}(n, \text{total})$ ,  $E = 3$  eV–76 keV; measured  $\sigma_t(E)$  to 76 keV; deduced resonance  $E_0$ ,  $g\Gamma_n^0$ ,  $D_0$ ,  $S_0$ ,  $S_1$ . ]

### I. INTRODUCTION

This is one of a series<sup>1</sup> of papers reporting results of high resolution neutron time of flight spectroscopy measurements using the Columbia University Nevis synchrocyclotron as a pulsed neutron source. Results are presented from 202.05 m transmission measurements and 39.57 m capture measurements using three different thickness samples of natural lanthanum, which is 99.91%  $^{139}\text{La}$  and 0.089%  $^{138}\text{La}$ , so it is essentially pure  $^{139}\text{La}$ . Results are presented of the measured  $\sigma_t$  vs  $E$  to about 75 keV and level energies and  $g\Gamma_n^0$  values are given for all observed levels below 26 keV, which are now believed to be due to  $^{139}\text{La}$ , treating them (arbitrarily) as  $s$  levels ( $l=0$ ). The observation of weaker  $l=1$  levels was complicated by the presence of a few times 0.1% natural erbium in the thick sample, and probably  $\sim 0.1\%$  Ta. After excluding weak levels which are known resonances in the erbium isotopes<sup>2</sup> or in Ta, most of the weak resonances previously reported<sup>3</sup> as possibly being due to  $^{139}\text{La}$  below 248 eV are now eliminated as probable  $^{139}\text{La}$  levels.

$^{139}\text{La}$  is of interest since, like  $^{142}\text{Nd}$ ,  $^{141}\text{Pr}$ , and  $^{140}\text{Ce}$ , it has closed shell neutron number 82. As with our results<sup>4</sup> for  $^{141}\text{Pr}$ , there are strong suggestions of intermediate structure effects. The plot of  $\sum g\Gamma_n^0$  vs  $E$  deviates from a straight line more than expected for a Porter-Thomas distribution, particularly below  $\sim 5$  keV. Similar effects are present for our (unpublished)  $^{140}\text{Ce}$  results as well as for our  $^{141}\text{Pr}$  results. One expects such intermediate structure effects to be most prominent for nuclei having nearly closed shells.

$^{139}\text{La}$  is also of interest in that it comes near the transition region between the low  $s$ -wave strength function,  $S_0$ , nuclei below  $A \sim 140$  and those in the rare earth region,  $A > 140$ , of the split  $4s$  peak in  $S_0$  vs  $A$ . Since it has a closed neutron shell, the average  $s$  level spacing is much greater than for somewhat lighter (iodine or cesium) or somewhat heavier (Sm or Eu) nuclei.

The main published results for  $^{139}\text{La}$  since 1960, besides the partial inclusion of our preliminary results in BNL 325,<sup>5</sup> are those of Shwe, Coté, and Prestwich<sup>6</sup> (Argonne 1967), and of Morgenstern, Alves, Julien, and Samour<sup>7</sup> (Saclay 1969), in addition to earlier Nevis results of Garg *et al.* which our present results supersede. The Argonne studies<sup>6</sup> used pure samples of  $\text{La}_2\text{O}_3$  and used  $\geq 11$  ns/m resolution fast chopper measurements. They give a plot of  $\sigma_t$  vs  $E$  from  $10^{-1}$  eV to 3 keV. Their between level cross sections are several barns lower than ours, and than earlier measurements for La above a few eV. The Saclay group<sup>7</sup> used three different thickness samples of  $\text{La}_2\text{O}_3$ , using  $\approx 1$  ns/m resolution. They do not present results for  $\sigma_t$  vs  $E$ , but give resonance partial neutron widths  $g\Gamma_n$  for about 70 resonances to 10.35 keV. Our results are in fairly good agreement with the Saclay  $g\Gamma_n^0$  values.

The detailed data analysis reported in this paper is mainly due to G. Hacken.

### II. EXPERIMENTAL DETAILS AND ANALYSIS PROCEDURES

These measurements for La were made during the same cyclotron "run" and with the same operating conditions as for our previously reported<sup>1</sup>

Er, Yb, In, W, and Gd measurements. The accelerator operated at 70 bursts/sec. We used our 202.05 m flight path for transmission measurements and the 39.57 m path for capture measurements. The reported cross section and resonance parameter results are based almost entirely on the transmission measurements. Three sample thicknesses were used. The thick sample of La metal had  $1/n = 13.9$  b/atom and provided the main information for between level  $\sigma_t$  vs  $E$  evaluations. It was the least pure of the samples, having a few  $\times 0.1\%$  of Er and Ta. The much purer medium thickness sample of  $\text{La}_2\text{O}_3$  had  $1/n = 50.5$  b/atom of La, while the thin sample had  $1/n = 227$  b/atom of La. The transmission measurements used three different time delays for the start of the 8192 detection channels. The "low energy" measurements covered from 21.2 to 2281 eV. The "medium energy" measurements covered from 570 eV to 21.3 keV, and the "high energy" region covered from 678 eV to 89.4 keV. The capture measurements covered from 3.1 eV to 3.2 keV. Measurements using the thick La sample used about 400 000 accelerator bursts for each of the four operating modes. The capture measurements also used 400 000 bursts each for the medium and thin samples. The low, medium, and high energy measurements used  $3 \times 10^5$ ,  $2 \times 10^5$ , and  $4 \times 10^5$  bursts for the medium sample and  $3 \times 10^5$ , zero, and  $3 \times 10^5$  bursts for the thin sample.

The capture measurements for the thick sample showed a very large number of resonances due to the  $< 1\%$  total impurities of the erbium isotopes and Ta. About 31 such peaks, not due to  $^{139}\text{La}$ , were seen below 100 eV. The medium  $\text{La}_2\text{O}_3$  sample capture results were free of Er and Ta resonances and showed many of the known reported resonances<sup>5</sup> in  $^{139}\text{La}$ , which is only 0.089% abundant in natural La.

The processing to analyze the thick, medium, and thin La data also used "open beam" measurements. The thick sample had essentially bottoming,  $T = 0$ , transmission dips at the strong 72, 1180, 2116, 2998, and 3485 eV levels. The medium sample had bottoming dips at the 72, 1180, and 2998 eV levels. The thin sample only had a bottoming dip at the 72 eV level (low energy data only). These bottoming dips were used to establish the background subtraction at these energies and seemed to be of the form of a constant plus a term of the form  $E^\alpha$ , different for each thickness. After background subtraction, and relative normalization to equal numbers of monitor counts, the ratio of medium to thick sample counts, particularly adjacent to these bottoming levels, gave transmission values,  $T$ , due to the difference

of the thickness, and thus the implied transmission for each thickness and the implied background subtracted open count. Similar procedures were used for the other energy region measurements, where the strong levels at 2997.5 and 3481.8 eV also gave extra  $T = 0$  information. The high, medium, and low energy  $(T, \sigma)$  values were averaged in their overlap energy region to obtain less statistical fluctuation for plotting  $\sigma_t$  vs  $E$ . The  $(T, \sigma)$  values for the three energy regions agreed to within statistical fluctuations in their overlap regions. In plotting  $\sigma_t$  vs  $E$  in Fig. 1, we only use the thick sample (metal) values except at resonances. Medium and thin sample cross sections are shown at resonances where appropriate, using different symbols for the points. Below  $\sim 7$  keV, we use up to 81 channel averages to reduce the point clutter and the between level statistical fluctuation effect. The "measured"  $\sigma_t$  vs  $E$  may differ appreciably from the "true"  $\sigma_t$  vs  $E$  values at resonances due to resolution effects and a limited range of sample thicknesses.

The analysis for resonance  $g\Gamma_n^0$  values was almost entirely based on our standard resonance dip "area" analysis<sup>2</sup> which is independent of measurement resolution and corrects for Doppler level broadening. Where more than one thickness data gave well defined implied results for  $g\Gamma_n$  vs  $\Gamma$ , the results were generally in good agreement at the intersection with the line  $\Gamma = 2g\Gamma_n + \langle \Gamma_\gamma \rangle$ , using  $\langle \Gamma_\gamma \rangle = 60$  meV. Since the  $^{139}\text{La}$  spin is  $\frac{7}{2}$ , we make no serious attempt to establish  $\Gamma_\gamma$  values or  $J$  values for the resonances, except for the 72.2 eV level which gave  $\Gamma_\gamma = (60 \pm 15)$  eV where some "shape" analysis could be used effectively.

The results for the resonance energies and  $g\Gamma_n^0$  values for  $^{139}\text{La}$  levels to 26 keV are given in Table I. Most very weak "levels" below  $\sim 1$  keV have been excluded because they are due to known levels in the Er isotopes, or to Ta or  $^{138}\text{La}$ . All levels in Table I were analyzed as if they were  $s$  levels.

### III. SYSTEMATICS OF THE RESULTS

Figure 2 shows a plot of the cumulative number of levels,  $N$ , in Table I vs  $E$ . Figure 3 shows a plot of  $\sum g\Gamma_n^0$  vs  $E$ . Figure 4 shows the histogram distribution for  $(g\Gamma_n^0)^{1/2}$  and comparisons with the single channel Porter-Thomas distribution curve based on 125  $s$  levels in 26 keV having  $s$ -wave strength function  $10^4 S_0 = 0.76$ , the mean slope of Fig. 3 to 26 keV.

From about 6 to 18 keV, Fig. 3 shows reasonably constant slope corresponding to  $10^4 S_0 \approx 0.50$ . The slope averages quite low until the two strong levels near 2998 and 3485 eV are reached; these

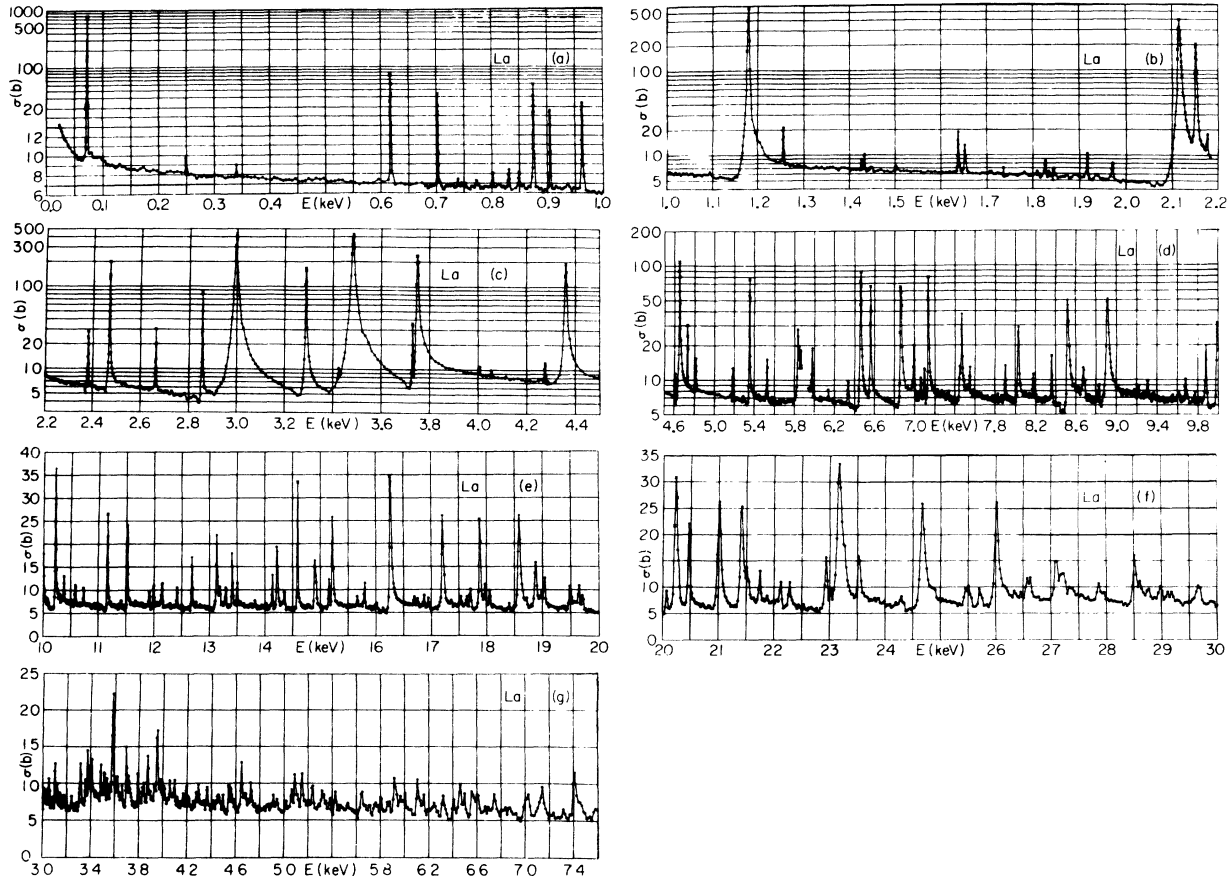


FIG. 1. The measured total cross section of natural La vs energy. (a) Below 1 keV. The points use up to 81 channel averages of the counts to obtain less statistical fluctuations and to avoid having too many  $\sigma_t$  points. At resonances fewer channel averages were used based on studying the results. The  $\sigma_t$  scale is linear from 6 to 14 b/atom and logarithmic above 14 b. (b) Results from 1 to 2.2 keV. (c) 2.2 to 4.5 keV. (d) 4.5 to 10 keV. The Al resonance at 5.9 keV prevents evaluations near that energy. Every channel is plotted above about 7 keV. (e) 10 to 20 keV. (f) 20 to 30 keV. (g) 30 to 76 keV. The thick, medium, and thin sample  $\sigma_t$  values are shown by  $\bullet$ ,  $+$ , and  $\times$ , respectively, with other than thick sample values only shown at appropriate resonances.

behave like contributions from an intermediate structure peaking. The region 18.5 to 26 keV gives an abnormally large slope contribution suggesting another intermediate structure peaking. Reference to Fig. 1, noting mainly the level widths in addition to the peak measured  $\sigma$  values, suggests a reduced rate of contribution from 26 to 33 keV and an anomalously larger contribution from the 33 to 40 keV region. Certainly Fig. 3 looks quite different from the similar plots for the  $A = 150$  to 190 region.

For our final estimate of the  $s$  level density for  $^{139}\text{La}$  as 125 levels to 26 keV ( $D_0 = 208$  eV) and  $10^4 S_0 = 0.76$ , the full curve in Fig. 4 shows the comparison of the predicted Porter-Thomas single channel distribution with the histogram for all levels. There is an excess of observed weak levels in the first histogram box, and approxi-

mately two extra observed levels in the last histogram box. We also show, for comparison, dashed, the histogram for the 6–26 keV region with the fit curve lowered by the ratio of the energy intervals. This eliminates most of the apparent excess of weak levels and the two very strong levels at 2998 and 3485 eV. The first two boxes are now a little above the fit curve and the fourth box is a little low, with a fair agreement elsewhere.

Although the likelihood of intermediate structure effects, as discussed above, complicates use of our usual analysis methods,<sup>2</sup> we have carried them out anyhow to help our understanding. This analysis assumed equal strength functions for the  $J = 3$  and 4  $s$  level populations. An intrinsic  $p$  level density twice the  $s$  level density was assumed, and calculations were made for  $10^4 S_0 = 0.76$  and for various choices of  $10^4 S_1$ . We stud-

TABLE I. Resonance parameters  $E_0$  and  $g\Gamma_n^0 = g\Gamma_n(1 \text{ eV}/E_0)^{1/2}$  for  $^{139}\text{La}$ . An asterisk following the  $g\Gamma_n^0$  value indicates that the level has  $>0.6$  Bayes probability for being a  $p$  level, based on  $10^4 S_1 = 0.6$ .

$E_0$ (eV)	$g\Gamma_n^0$ (meV)	$E_0$ (eV)	$g\Gamma_n^0$ (meV)	$E_0$ (eV)	$g\Gamma_n^0$ (meV)	$E_0$ (eV)	$g\Gamma_n^0$ (meV)
72.3+0.1	1.77 +0.05	4817.5+2.3	1.1 +0.2	10050+ 7	0.12+0.09*	17362+16	1.1+ 0.9*
248.2+0.2	0.006+0.002*	5185.2+2.5	0.9 +0.1 *	10071+ 7	0.4 +0.3 *	17536+16	6.2+ 3.8
339.4+0.2	0.006+0.004*	5352.8+2.7	8.2 +1.5	10221+ 7	24 +3	17648+16	2.0+ 1.5*
617.4+0.2	0.60 +0.03	5528.5+2.8	1.7 +0.2	10303+ 7	0.6 +0.4 *	17712+16	8.3+ 3.5
702.5+0.2	0.15 +0.02 *	5833.2+3.0	7.9 +4.0	10379+ 7	2.9 +1.5	17874+16	30 + 8
875.5+0.4	0.39 +0.05	5845.5+3.0	1.0 +0.7 *	10588+ 7	2.8 +0.3	17973+16	6.8+ 2.4
905.3+0.4	0.12 +0.03 *	5860.8+3.1	0.9 +0.5 *	10739+ 8	3.0 +0.6	18056+17	7.4+ 2.0
962.8+0.4	0.28 +0.02	5979.3+3.2	3.7 +0.6	11171+ 8	8.5 +1.5	18410+17	1.7+ 0.9*
1178.7+0.5	26.9 +1.0	6336.4+3.5	1.2 +0.6 *	11417+ 8	0.5 +0.4 *	18582+17	62 +16
1208.0+0.6	0.20 +0.04 *	6462.5+3.6	26 +3	11526+ 8	13 +3	18721+18	1.0+ 0.8*
1256.3+0.6	0.31 +0.05 *	6559.6+3.6	9.3 +1.8	11917+ 9	2.4 +0.7	18880+18	29 +10
1426.3+0.7	0.04 +0.01 *	6864.4+3.9	22 +2	11998+ 9	3.3 +1.0	18987+18	1.8+ 1.4*
1433.0+0.7	0.07 +0.02 *	6990.7+4.0	7.2 +0.8	12152+ 9	8.3 +2.1	19041+18	19 + 6
1637.5+0.9	0.35 +0.05 *	7061.3+4.1	0.8 +0.2 *	12413+ 9	5.2 +1.0	19480+19	11.8+ 3.0
1652.1+0.9	0.21 +0.03 *	7100.0+4.1	1.6 +0.3	12688+10	8.5 +2.5	19649+19	8 + 4
1826.4+0.5	0.08 +0.02 *	7137.0+4.1	15.4 +5.0	13134+10	22 +5	19705+19	4.6+ 2.1
1916.7+0.6	0.14 +0.05 *	7448.2+4.4	1.5 +1.0	13186+10	3.0 +1.0	20070+19	9.9+ 3.7
1971.3+0.6	0.10 +0.02 *	7466.0+4.4	11.6 +6.0	13290+10	7.4 +0.8	20227+20	60 +15
2116.0+0.6	37 +4	7550.4+4.5	1.5 +0.3	13406+11	9.4 +1.7	20266+20	6 + 4
2151.7+0.7	10.4 +0.7	7903.7+4.8	2.0 +0.5	13497+11	6.4 +1.0	20465+20	29 +18
2176.5+0.7	0.21 +0.02 *	8035.2+4.9	14.5 +3.5	13820+11	0.7 +0.4 *	21017+21	69 +21
2381.1+0.8	0.70 +0.05	8180.1+5.1	1.5 +0.3 *	14022+11	0.8 +0.5 *	21409+21	60 +30
2469.8+0.8	10.3 +1.5	8362.9+5.2	2.5 +0.7	14136+12	7.6 +2.3	21505+22	15 + 8
2666.0+1.0	0.7 +0.1	8519.5+5.4	27 +3	14217+12	17.8 +3.3	21745+22	15.6+ 3.9
2856.6+1.0	3.7 +0.4	8672.3+5.5	4 +2	14352+12	7.1 +2.0	21877+22	2 + 2 *
2997.5+1.1	105 +7	8688.9+5.5	1.3 +0.7 *	14584+12	16.6 +2.5	22123+23	11 + 4
3287.7+1.3	18 +3	8834.9+5.7	0.96+0.10*	14902+12	20.7 +4.5	22281+23	20 + 5
3424.8+1.4	0.17 +0.09 *	8915.0+5.8	39 +5	15155+13	5.0 +0.8	22933+24	26 +13
3484.6+1.4	122 +6	9219.3+6.1	0.5 +0.3 *	15219+13	24 +8	23016+24	2.5+ 2.0*
3729.1+1.6	1.5 +0.3	9310.9+6.1	1.0 +0.3 *	15665+13	1.8 +1.2 *	23172+24	100 +45
3749.4+1.6	42 +4	9610.1+6.5	0.5 +0.3 *	15800+14	7.2 +1.5	23269+24	30 +20
4008.9+1.7	0.2 +0.2 *	9681.4+6.5	1.7 +0.8 *	16020+14	3.5 +3.1	23514+25	33 +10
4275.2+1.9	0.44 +0.12 *	9770.0+6.6	0.6 +0.4 *	16132+14	0.8 +0.5 *	24285+26	2.1+ 1.9*
4360.6+2.0	38 +3	9826.5+6.7	0.34+0.17*	16273+14	57 +9	24666+27	90 +25
4613.6+2.1	0.6 +0.2 *	9880.0+6.7	6.2 +0.8	16693+15	1.5 +0.9 *	24826+27	5 + 3
4650.3+2.2	26 +3	9991.9+6.8	20.3 +2.5	16745+15	3.4 +2.0	25509+28	36 +13
4729.4+2.2	0.75 +0.25 *			16872+15	4.0 +2.5	25705+28	13 + 4
				16947+15	3.6 +3.0	26018+29	99 +30
				17207+15	35 +8		

ied our analysis for resonances which have  $g\Gamma_n/E$  about  $5.2 (E/1 \text{ eV})^{0.78} \times 10^{-9}$ . The probable number of missed  $s$  levels vs  $E$  was calculated, and so was the expected number of detected  $p$  levels vs  $E$ . The calculated values for number

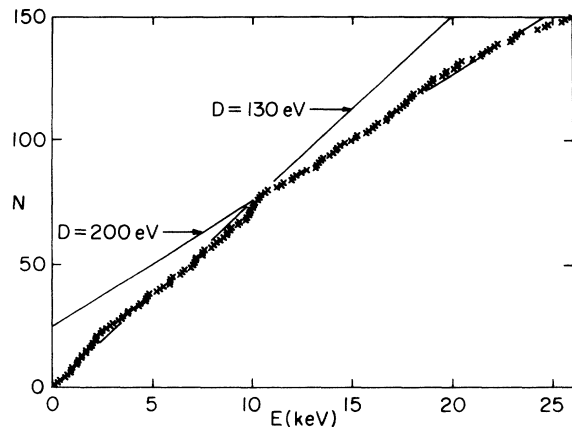


FIG. 2. Plot of observed number,  $N$ , of resonances vs the energy  $E$ . The two indicated slope lines are for mean level spacings 130 and 200 eV.

of detected  $p$  levels expected is reduced by a factor  $\approx 0.8$  to  $0.9$ , depending on  $E$ , to account for “shielding” effects of detected  $s$  levels. The results were that approximately two  $s$  levels were

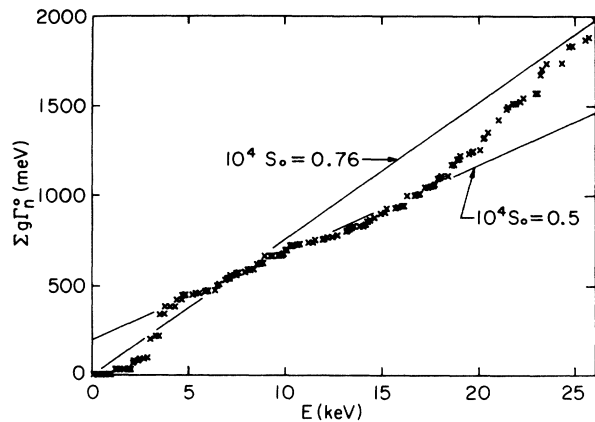


FIG. 3. Plot of  $\sum g\Gamma_n^0$  vs  $E$ . The slope corresponds to the  $s$ -wave strength function  $S_0$ . The average slope over the full region corresponds  $10^4 S_0 = 0.76$ , while that from 6 to 19 keV corresponds to  $10^4 S_0 = 0.50$ .

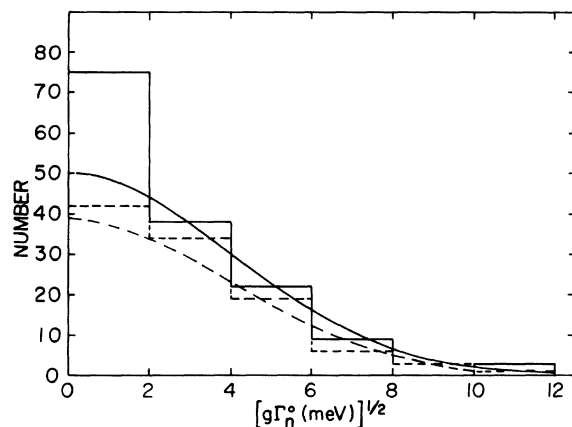


FIG. 4. Histogram of  $(g\Gamma_n^0)^{1/2}$  values compared with single channel Porter-Thomas distributions corresponding to  $10^4 S_1 = 0.76$  and 125 s levels/26 keV. The solid curve and histogram for the full region fits well except for an excess of weak levels and very strong levels (first and last histogram boxes). The dashed curve and histogram are for the region 6 to 26 keV. (The fifth histogram box is for both regions.)

probably missed to 6 keV, and 23 missed to 26 keV. This suggests that about  $150 - 125 + 23 = 48$  of the observed levels were  $p$  levels. For  $10^4 S_1 = 0.6$ , the expected number of detected  $p$  levels was 13, 18, and 50 to 4, 6, and 26 keV, respec-

tively. A Bayes' theorem analysis of the probability that a detected level  $g\Gamma_n^0$  value implied  $l=0$  or  $l=1$  gave 16, 21, and 52 for the sum of the  $p$  level probabilities to 4, 6, and 26 keV. This choice of  $S_1$  gave a much better match than higher or lower values to the expected number of  $p$  levels and to the Bayes  $\sum$  probability for  $p$  levels. For  $10^4 S_1 = 0.4$  and 0.9, the expected numbers of  $p$  levels to 26 keV were 29 and 74, while the Bayes sums of probability for  $p$  levels to 26 keV were 40 and 62, respectively. Thus, we choose  $0.4 < 10^4 S_1 < 0.9$ , with 0.6 favored. The calculations for  $S_1$  used a channel radius of  $1.4A^{1/3}$  fm. In Table I an asterisk after the  $g\Gamma_n^0$  value indicates  $>0.6$  probability that the level is  $l=1$  from a Bayes analysis with  $10^4 S_1 = 0.6$ . There are 50 such levels.

In conclusion, we note that intermediate structure effects seem to be present. There are probably approximately 50  $p$  levels observed, with those having asterisks after the  $g\Gamma_n^0$  in Table I having the highest Bayes' theorem probability of being  $p$  levels.

We thank Dr. H. S. Camarda, Dr. F. Rahn, Dr. M. Slagowitz, and Dr. S. Wynchank for their involvement in the measurements. C. Gillman and W. Marshall furnished important technical support.

\*Present address: Brookhaven National Laboratory, Upton, New York 11973.

†Research supported by U. S. Energy Research and Development Administration.

<sup>1</sup>References to all previous papers in this series can be found in U. N. Singh, J. Rainwater, H. I. Liou, G. Hacken, and J. B. Garg, Phys. Rev. C **13**, (1976), <sup>209</sup>Bi.

<sup>2</sup>H. I. Liou *et al.*, Phys. Rev. C **5**, 974 (1972), Er.

<sup>3</sup>G. Hacken, Ph.D. thesis, Columbia University, 1971 (unpublished).

<sup>4</sup>S. Wynchank, J. B. Garg, W. W. Havens, Jr., and

J. Rainwater, Phys. Rev. **166**, 1234 (1968), Mo, Sb, Te, Pr.

<sup>5</sup>*Neutron Resonance Parameters*, compiled by S. F. Mughabghab and D. I. Garber, Brookhaven National Laboratory Report BNL-325 (National Technical Information Service, Springfield, Virginia, 1973), 3rd. ed., Vol. I.

<sup>6</sup>H. Shwe, R. E. Coté, and W. V. Prestwich, Phys. Rev. **159**, 1050 (1967).

<sup>7</sup>J. Morgenstern, R. N. Alves, J. Julien, and C. Samour, Nucl. Phys. **A123**, 561 (1969).